

Prediction of Tetraoxygen Formation on Rutile TiO₂(110)

Devina Pillay, Yun Wang, and Gyeong S. Hwang*

Department of Chemical Engineering and Institute of Theoretical Chemistry, The University of Texas at Austin, Austin, Texas 78712

Received June 22, 2006; E-mail: gshwang@che.utexas.edu

The interaction of TiO₂ with molecular oxygen is an important factor in determining many fundamental reactions that take place on TiO₂-based materials.^{1–5} While adsorption of O₂ molecules is known to be mainly mediated by oxygen vacancies, the atomic structure and reactivity of adsorbed O₂ molecules on the reduced surface are still uncertain, particularly at saturation coverage. Results from recent temperature-programmed desorption (TPD) measurements^{6,7} suggested that the full O₂ coverage on TiO₂(110) at low temperature (~120 K) would approximately be 3 times the surface vacancy population, and adsorbed O₂ molecules may exist in either weakly or strongly bound states associated with TPD features below 200 K and above 400 K, respectively. In addition, earlier experiments⁸ identified the existence of two chemisorption states for molecular oxygen on TiO₂(110); that is, one can photo-oxidize coadsorbed CO and the other only undergoes fast photodesorption. Most of the recent theoretical studies using density functional theory (DFT) have focused on understanding the nature of O₂ interaction with the reduced surface, by examining the adsorption and dissociation of a single oxygen molecule per vacancy or more.^{9–11} In fact, on the basis of the unrestricted Hartree–Fock calculations, a structural model was proposed for adsorption of three O₂ molecules per vacancy, in which one O₂ molecule is located at the vacancy site while the others are at the sites atop adjacent Ti 5-fold-coordinated atoms, all in a perpendicular fashion.¹²

In this paper, we propose a new adsorption model for molecular oxygen on reduced TiO₂(110), based on extensive first principles density functional calculations of the structure, bonding, and energetics of adsorbed oxygen species by changing the number of adsorbed O₂ molecules per vacancy. For the first time, as shown in Figure 1, our calculations predict formation of tetraoxygen (O₄) anchored at the vacancy site, which in turn allows adsorption of three O₂ molecules per vacancy in saturation coverage. The O₄ complex turns out to be substantially more stable than two separately adsorbed O₂ molecules. We have also determined that thermally activated O₂ desorption would take place via two channels that require overcoming barriers of 0.41 and 1.25 eV, respectively. In addition, our study provides strong theoretical evidence for the change in O₂ reactivity with O₂ coverage. Our findings associated with tetraoxygen complexes are consistent with existing experimental results, as discussed below. The improved understanding will greatly assist in understanding and predicting a variety of chemical and photochemical processes occurring on TiO₂ surfaces.

Our density functional calculations were performed within the generalized gradient approximation (GGA-PW91), using a plane-wave basis set and Vanderbilt ultrasoft pseudopotentials, as implemented in the well-established Vienna ab initio Simulation Package (VASP). Given the importance of correct spin treatment for studying the behavior of oxygen species, all atomic structures and energies reported herein were calculated considering spin polarization. A planewave cutoff energy of 300 eV was used. For the Brillouin zone integration, we used a (2 × 4 × 1) Monkhost–

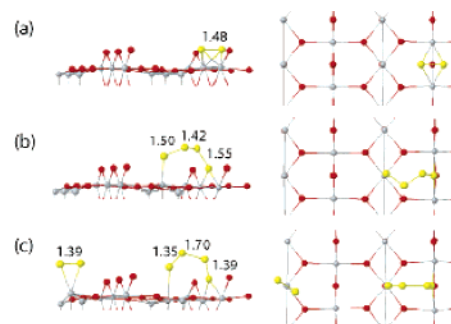


Figure 1. Side (left panel) and top (right panel) views of lowest-energy configurations of O₂ at varying coverages: (a) $\theta = 1$, (b) $\theta = 2$, and (c) $\theta = 3$, where θ is defined as the number of adsorbed O₂ molecules per oxygen vacancy. Bond lengths of oxygen species are given in Å. The yellow, red, and gray balls represent adsorbed O, surface O, and Ti atoms, respectively.

Pack mesh of k points. The nudged elastic band method (NEBM) was used to determine diffusion pathways and barriers. A reduced surface is generated by removing a bridging O atom from a 15-atomic layer (2 × 3) slab that is separated from its periodic images by a vacuum space of 10 Å. For gas-phase O₂, we used the same size of periodic computation box, sufficiently large to avoid possible interactions with its replicas. Note that the ground state of the gas-phase O₂ molecule is the triplet state, which was used as the reference state for binding energy prediction of oxygen adsorbates on the reduced surface. Our previous studies¹⁰ showed that the chosen conditions of spin-polarized DFT calculations are sufficient for describing the O₂–TiO₂(110) interaction.

For $\theta = 1$, that is, one O₂ adsorption per vacancy, the most favorable adsorption occurs when O₂ is positioned at the vacancy site in parallel fashion (Figure 1a). Electron delocalization from the vacancy site also renders stable adsorption sites for O₂ along neighboring Ti(5c) rows. The adsorbed O₂ may undergo migration along the Ti(5c) row, with a barrier of 0.54 eV, until reaching the lowest-energy configuration at the vacancy site by overcoming a barrier of 0.45 eV. The O₂ bond length of 1.48 Å, close to 1.46 Å for O₂²⁻ (in H₂O₂), indicates that approximately two electrons transfer from the surface to the adsorbed (singlet state) O₂ (see Figure 2a). The O₂²⁻ binding energy is predicted to be 2.72 eV, with respect to the gas-phase (triplet state) O₂.

When $\theta = 2$, as illustrated in Figure 1b, the most stable adsorption structure involves formation of a tetraoxygen (O₄) complex which is aligned between the O vacancy and an adjacent Ti(5c) atom. The O₄ binding energy is predicted to be 2.93 eV with respect to two gas-phase O₂ molecules in the triplet state. The O–O bond lengths in the O₄ complex are 1.50, 1.42, and 1.55 Å, between O1–O2, O2–O3, and O3–O4, respectively, where O1 is the O atom at the vacancy site, O2 the next nearest neighbor to the vacancy oxygen atom (O1), and O3 is between O2 and O4 (which is at the top site above the neighboring Ti(5c) atom). The atomic structure is similar to O₄²⁻ (in H₂O₄), which gives 1.50 and 1.45

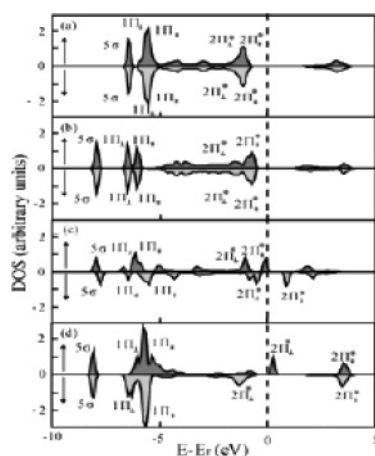


Figure 2. LDOS projected on (a) O_2^{2-} at the vacancy site when $\theta = 1$, (b) O_4^{2-} at the vacancy site when $\theta = 2$, (c) O_4^{-} at the vacancy site when $\theta = 3$, and (d) O_2^{-} at the Ti(5c) site when $\theta = 3$. Here, the Fermi level is positioned at the top of the collection of electron energy levels.

Å, respectively, for the corresponding O1–O2/O3–O4 and O2–O3 bond lengths. This indicates that approximately two electrons transfer to the O_4 complex from the vacancy site. We attribute the small discrepancy between the adsorbed and gas-phase O_4 complexes to the geometric constraint that the reduced surface imposes on the adsorbed one. The O_4^{2-} formation lowers the adsorption energy by 0.6–0.9 eV relative to two separately adsorbed O_2^{-} molecules in various configurations. The existence of tetraoxygen molecules in the gas phase has been theoretically predicted and also evidenced by recent experiments.¹³ While the shape of isolated O_4 molecules is still unclear, our DFT-GGA calculations are in good agreement with previous theoretical studies^{14–16} except for their bond lengths, which are likely to be somewhat sensitive to the choice of exchange-correlation functional.

Our calculation predicts that the dissociation of O_4^{2-} into two separately adsorbed O_2^{-} molecules, one in a parallel configuration above the vacancy site and the other diagonally adsorbed above the Ti(5c) site, requires overcoming a barrier of approximately 1.25 eV. It appears that the dissociation process is endothermic by 0.90 eV, and the O_2^{-} at the Ti(5c) site easily undergoes desorption (into triplet O_2) with a barrier of 0.30 eV.

As shown in Figure 1c, the formation of the O_4 complex allows adsorption of an additional O_2 molecule at a neighboring Ti(5c) site, resulting in three O_2 molecules adsorbed per vacancy ($\theta = 3$). The additional O_2 adsorption results in a noticeable change in the bonding configuration of O_4 ; that is, the O–O bond lengths become 1.35, 1.70, and 1.39 Å between O1–O2, O2–O3, and O3–O4, respectively. The atomic structure is virtually identical to that of a gas-phase O_4^{-} (in HO_4) in which the corresponding O1–O2, O2–O3, and O3–O4 lengths are 1.32, 1.79, and 1.41 Å, respectively. The gas-phase O_4^{-} geometry agrees well with previous theoretical results.¹⁴ We have also found that the bond length of the third O_2 above the Ti(5c) atom is 1.39 Å, close to 1.37 Å for O_2^{-} (in HO_2). The bond length variation indicates that an electron is transferred from the surface to each of the O_2 and O_4 molecules, also evidenced by their density of states (Figure 2). The barrier for desorption of the third O_2^{-} (into triplet O_2 in the gas phase) is predicted to be 0.41 eV.

For the sake of completeness, we also considered a surface with two vacancies and six O_2 molecules, allowing the formation of three O_4 complexes; that is, two are in the vacancy sites and one is aligned along the Ti(5c) row. However, the O_4 complex along the Ti(5c)

row is energetically degenerate to two separate O_2 molecules adsorbed along the Ti(5c) row. Additionally, we examined adsorption of four O_2 molecules per vacancy by placing one O_4 complex along the Ti(5c) row and another O_4 complex atop the O vacancy site, but it turns out to be unlikely.

Figure 2 shows the spectra of the local density of states (LDOS) projected on the adsorbed oxygen species, which can also demonstrate the activation of adsorbed O_2 molecules via charge transfer from the reduced TiO_2 surface. The full spin-manifold of the antibonding $2\pi^*$ states of O_2^{2-} (at $\theta = 1$) and O_4^{2-} (at $\theta = 2$) is located below the Fermi energy (E_F). The filling of the antibonding orbitals results in a strong activation of the oxygen species. On the other hand, at $\theta = 3$, the LDOS spectra show that the O $2\pi^*$ bands shift significantly higher in energy, but the spin-down $2\pi^*_{\perp}$ state is still slightly below E_F . This indicates that the activation of O_2^{-} and O_4^{-} species (at $\theta = 3$) is attributed to occupation of the $2\pi^*_{\perp}$ orbital, albeit not as strong as when $\theta \leq 2$.

Our calculation results clearly show that an oxygen vacancy can be responsible for adsorption of up to three O_2 molecules on TiO_2 -(110), consistent with recent TPD measurements.⁷ From the saturation coverage ($\theta = 3$), O_2 desorption is predicted to occur via two channels, that is, (i) desorption off of the Ti(5c) site with a barrier of 0.41 eV and (ii) dissociation of O_4 into two separately adsorbed O_2 molecules (one above the vacancy site and the other atop a Ti(5c) atom), followed by desorption of the latter, which requires overcoming an overall activation barrier of 1.25 eV. The desorption energies are in excellent agreement with TPD features^{6,7} that appear at 145 K (or 164 K) and 410 K (or 416 K), corresponding to O_2 binding energies of 0.35 eV (or 0.44 eV) and 1.14 eV (or 1.25) eV, respectively. Additionally, our study shows that there exist O_2 and O_4 species at various charge states, depending on the relative population of adsorbed O_2 molecules versus oxygen vacancies. This led us to speculate that, to some degree, the coverage-dependent behavior may be responsible for the reactivity change of O_2 toward photoinduced CO oxidation as identified by earlier experiments,⁸ warranting a further theoretical study of photoinduced desorption of and CO oxidation by these O_2 and O_4 species at various charge states.

Acknowledgment. The authors acknowledge the Welch Foundation (F-1535) for their financial support of this work.

References

- (1) Fox, M. A.; Dulay, M. T. *Chem. Rev.* **1993**, *93*, 341–357.
- (2) Diebold, U.; Lehman, J.; Mahmoud, T.; Kuhn, M.; Leonardelli, G.; Hebenstreit, W.; Schmid, M.; Varga, P. *Surf. Sci.* **1998**, *411*, 137–153.
- (3) Linsebigler, A. L.; Lu, G. Q.; Yates, J. T. *Chem. Rev.* **1995**, *95*, 735–758.
- (4) Campbell, C. T.; Parker, S. C.; Starr, D. E. *Science* **2002**, *298*, 811–814.
- (5) Lai, X. F.; Goodman, D. W. *J. Mol. Catal. A* **2000**, *162*, 33–50.
- (6) Beck, D. D.; White, J. M.; Ratcliffe, C. T. *J. Phys. Chem.* **1986**, *90*, 3132–3136.
- (7) Henderson, M. A.; Epling, W. S.; Perkins, C. L.; Peden, C. H. F.; Diebold, U. *J. Phys. Chem. B* **1999**, *103*, 5328–5337.
- (8) Lu, G. Q.; Linsebigler, A.; Yates, J. T. *J. Chem. Phys.* **1995**, *102*, 3005–3008.
- (9) Rasmussen, M. D.; Molina, L. M.; Hammer, B. *J. Chem. Phys.* **2004**, *120*, 988–997.
- (10) Wang, Y.; Pillay, D.; Hwang, G. S. *Phys. Rev. B* **2004**, *70*, 193410.
- (11) Wu, X. Y.; Selloni, A.; Lazzeri, M.; Nayak, S. K. *Phys. Rev. B* **2003**, *68*, 241401.
- (12) de Lara-Castells, M. P.; Krause, J. L. *Chem. Phys. Lett.* **2002**, *354*, 483–490.
- (13) Cacace, F.; de Petris, G.; Troiani, A. *Angew. Chem., Int. Ed.* **2001**, *40*, 4062.
- (14) Chertihin, G. V.; Andrews, L. *J. Chem. Phys.* **1998**, *108*, 6404–6407.
- (15) Fermann, J. T.; Hoffman, B. C.; Tschumper, G. S.; Schaefer, H. F. *J. Chem. Phys.* **1997**, *106*, 5102–5108.
- (16) Xu, X.; Muller, R. P.; Goddard, W. A. *Proc. Natl. Acad. Sci. U.S.A.* **2002**, *99*, 3376–3381.

JA063453Y